

Characterization of the anticancer effect of mebendazole and its interaction with standard cytotoxic drugs in patient tumor cells *ex vivo* and in an *in vivo* mouse model

SHARMINEH MANSOORI¹, KRISTIN BLOM¹, CLAES ANDERSSON¹,
MÅRTEN FRYKNÄS¹, ROLF LARSSON¹ and PETER NYGREN²

¹Department of Medical Sciences, Akademiska Hospital (Uppsala University Hospital), 751 85 Uppsala, Sweden;

²Department of Immunology, Genetics and Pathology, Uppsala University, 751 85 Uppsala, Sweden

Received September 4, 2024; Accepted September 25, 2025

DOI: 10.3892/or.2025.9014

Abstract. Mebendazole (Mbz), a well-known anthelmintic drug, has demonstrated anticancer properties in tumor models and patients, and is thus under consideration for repositioning into an anticancer drug. Mbz is directly cytotoxic in cell lines by various mechanisms and acts indirectly via immunomodulation. In the present study, the anticancer effects of Mbz, alone and in combination with cytotoxic drugs, were further characterized using primary cultures of patient tumor cells *ex vivo* and the murine colon cancer cell line, CT26, *in vitro* and *in vivo*. Patient-derived tumor cells from acute myeloid leukemia (AML) and ovarian, colorectal and renal cancer were exposed to Mbz alone and, for solid tumors and the CT26 cell line, in combination with irinotecan, cisplatin or gemcitabine (patient cells only). Cytotoxicity was assessed using the fluorometric microculture cytotoxicity assay. *In vivo*, the antitumor effects of Mbz and irinotecan, alone and in combination, were evaluated in the BALB/c CT26 colon cancer mouse model by tumor growth measurements and flow cytometric analysis of tumor immune cell infiltration. In the patient cell samples, Mbz showed modest single-agent cytotoxicity, with the AML samples being the most sensitive, and displayed enhanced effects when combined with cytotoxic drugs, particularly irinotecan. CT26 cells showed modest dose-independent sensitivity to Mbz, which enhanced the effect of both cisplatin and irinotecan. *In vivo*, Mbz and irinotecan both inhibited tumor growth, but the combination did not significantly outperform Mbz alone. Flow cytometry of the resected mouse tumors indicated that Mbz promoted macrophage polarization from the M2 to M1 phenotype, suggesting that immune modulation

may contribute to its anticancer effect. Mbz has features making it a candidate for repositioning into an anticancer drug and part of its effect may be mediated by macrophage modulation.

Introduction

Mebendazole (Mbz), a broad-spectrum anthelmintic drug, is widely used to treat various helminthic infections but has also shown anticancer activity (1). In preclinical models, Mbz induces dose-dependent direct cytotoxic effects in adrenocortical carcinoma, lung cancer, melanoma, ovarian cancer and glioblastoma (2-7). Furthermore, arrest of tumor growth has been observed in cancer xenograft mouse models (2-5,8). Clinically meaningful activity of Mbz has also been reported in two case reports of patients with colorectal cancer (CRC) and adrenocortical carcinoma (9,10). The anticancer properties of Mbz have been proposed to be due to direct cytotoxic actions such as tubulin polymerization inhibition (6), protein kinase inhibition (11), anti-angiogenesis (12) and inhibition of the Hedgehog pathway (13). More recently, we observed that Mbz also induces an antitumoral immune response *ex vivo* by activation of M1 macrophages through the ERK I/II and Toll-like receptor-8 dependent pathway (14,15) along with induction of pro-inflammatory cytokines (16).

The concept of administering a combination of two or more anticancer drugs has been a cornerstone in cancer therapy. This approach generally enhances the treatment efficacy and reduces drug resistance (17,18). Traditionally, anticancer drug combinations have been identified through empirical screening for non-overlapping toxicities, whereas contemporary strategies increasingly employ mechanistic rationales for which drugs to combine (19,20). Preclinical studies frequently report synergistic interactions when combining drugs, whereas such interactions hardly apply in the clinic (21). Additive or sub-additive interactions are more realistic effects to expect and would still provide clinical benefits (22).

Combinations of Mbz with established anticancer drugs have been explored in cell line models. For example, in a melanoma cell line, Mbz increases apoptosis when combined with trametinib (23). Similarly, synergistic effects have been

Correspondence to: Dr Sharminah Mansoori, Department of Medical Sciences, Akademiska Hospital (Uppsala University Hospital), Dag Hammarskjölds väg 8, 751 85 Uppsala, Sweden
E-mail: sharminah.mansoori@medsci.uu.se

Key words: drug repositioning, mebendazole, cancer, *ex vivo*, *in vivo*

observed when Mbz is combined with temozolomide and vincristine or with gemcitabine in brain and breast cancer cell lines, respectively (24,25). We previously found single drug Mbz administration to be ineffective in patients with advanced previously treated gastrointestinal cancer (26). However, in early clinical studies of glioblastoma and CRC, combining Mbz with chemotherapy was found to be safe and appeared to provide patient benefit (27-30).

With this background, we considered it relevant to further characterize the anticancer properties of single agent Mbz and Mbz in combination with irinotecan, gemcitabine and cisplatin in a clinically relevant *ex vivo* model of primary cultures of patient tumor cells as well as *in vivo* with a murine colon cancer model. These cytotoxic drugs were selected based on their well-characterized mechanisms of action (31), allowing for the assessment of whether Mbz exhibits broad-spectrum synergy or if its interactions are specific to certain drug classes. Moreover, all three agents are standard-of-care therapies for several solid tumors (31). The study was designed to address certain critical gaps in the research on Mbz as a potential anticancer drug, mainly its cytotoxic activity as a single drug, its interaction with standard cytotoxic anticancer drugs and its modes of action. This motivated the use of a somewhat mixed study design using clinically relevant *ex vivo* human tumor models as well as an immune-competent *in vivo* colon cancer model.

Materials and methods

Preparation of patient tumor cells for ex vivo assessment of direct cytotoxicity. Tumor samples were obtained from adult patients aged ≥ 18 years with acute myeloid leukemia (AML) or colorectal, ovarian or renal cancer at Akademiska Hospital (Uppsala University Hospital) (Uppsala, Sweden) by bone marrow or peripheral blood sampling, intraoperatively or by diagnostic biopsy in accordance with the approval from the Regional Ethical Committee in Uppsala (approval no. 2007/237). The samples were collected January 2008-December 2014, prepared as detailed below and then cryopreserved until use in 2022 for experiments in the present study. Written informed consent for sample collection and further analysis was provided by patients before sampling. Inclusion criteria for sampling were: i) Patients aged ≥ 18 years; ii) localized or advanced untreated or previously treated disease; and iii) the sampling procedure was considered to be safe and with a prospect that drug sensitivity testing could be of potential patient benefit. Sex distribution among the included patients was 70% (n=155) women and 30% (n=67) men.

The cell preparation protocol for solid and leukemic tumors has been described in detail elsewhere (32). Briefly, for the solid tumors, the samples were manually minced using sterile scissors and dispersed in collagenase [collagenase type I, 1.5 mg/ml (Sigma-Aldrich; Merck KGaA) and DNase type I, 100 μ g/ml (Sigma-Aldrich; Merck KGaA) in CO₂ Independent Medium, pH 7.35-7.45 (Gibco; Thermo Fisher Scientific, Inc.)] for 4 h at 37°C. The samples were then purified by density gradient centrifugation [200 x g, 5 min, at room temperature (RT)] (Histopaque®-1077; Sigma-Aldrich; Merck KGaA) followed by the determination of cell viability and count using a Bürker chamber. The cells were diluted in complete culture medium

[RPMI 1640 (Thermo Fisher Scientific, Inc.) containing 10% fetal calf serum (Sigma-Aldrich; Merck KGaA) and 2% glutamine/penicillin-streptomycin] in a 37°C humidified atmosphere containing 5% CO₂ before seeding in plates for further analysis.

The leukemic cells were isolated by Ficoll-Paque density gradient centrifugation (400 x g, 30 min, RT) and then counted using a Bürker chamber after staining for viability in Türk's solution (33). The cells were then diluted in complete culture medium until experimental seeding.

Isolated cells were stained using the May-Grünwald Giemsa staining method. Cells were placed on slides then first stained with May-Grünwald solution for 5 min at RT, washed thoroughly in deionized water and then stained in Giemsa solution for 10 min at RT, followed by another wash. Slides were air-dried and evaluated for tumor representativity, based on cell size, nucleus to cytoplasm ratio, chromatin staining pattern, presence of nucleoli and mitoses and cellular adhesion tendency, by a trained cytopathologist. A representative image of May-grünwald Giemsa stained isolated cells from a colorectal tumor is shown in Fig. 1. Only samples with $\geq 70\%$ tumor cells were included in the study.

Assessment of direct cellular toxicity in patient tumor cells. The fluorometric microculture cytotoxicity assay (FMCA) described in detail previously (34), was used for the measurement of cell survival. In the FMCA, living cells with an intact membrane hydrolyze fluorescein diacetate to fluorescein. By measuring fluorescence, cell survival is expressed as the survival index % (SI), calculated as: $SI = (F_{\text{sample}} - F_{\text{blank}}) / (F_{\text{control}} - F_{\text{blank}}) \times 100$, where F_{sample} represents the fluorescence in wells with the drug, F_{control} the fluorescence in wells with cells and medium and F_{blank} the fluorescence in wells with medium alone. The FMCA is a total cell death assay, the results of which correspond well with the much more laborious clonogenic assay (35).

Briefly, 5,000 cells/well (solid tumor samples), or 20,000 cells/well (hematological tumor samples) were seeded in 384-well Nunc culture plates (cat. no. 164688; Thermo Fisher Scientific, Inc.) using the pipetting robot, Biomek 4000 (Beckman Coulter, Inc.). Drugs were added immediately after cell seeding using an ECHO 550 system (Beckman Coulter, Inc.). The plates were incubated for 72 h in a 37°C humidified atmosphere containing 5% CO₂ and then transferred to an integrated system for automated fluorescence scanning and data calculation. A successful assay was defined by a fluorescence signal in control wells of ≥ 5 times the mean blank and a coefficient of variation of cell survival in control cultures of ≤ 30 and $\geq 70\%$ tumor cells before incubation and/or on the assay day.

Mbz was purchased from Sigma-Aldrich (Merck KGaA) whereas cisplatin, irinotecan and gemcitabine were either from commercial clinical preparations or obtained from Selleck Chemicals or LC Laboratories. Mbz was tested at concentrations of 45, 15, 5, 1.67 and 0.56 μ M, cisplatin at 30, 10, 3.3, 1.12 and 0.37 μ M, irinotecan at 180, 60, 20, 6.6 and 2.2 μ M, and gemcitabine at 90, 30, 10, 3.34 and 1.12 μ M. The procedure of drug dissolution and storage has been described in detail by Blom *et al* (32).

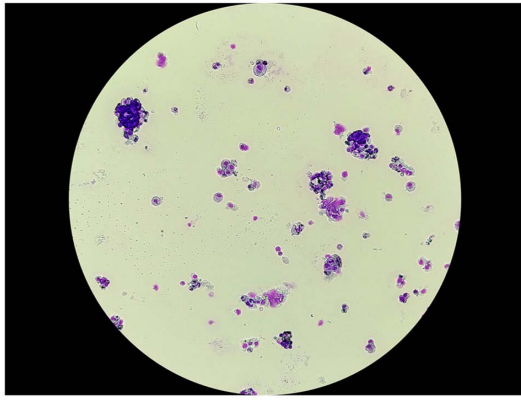


Figure 1. Representative image of May-Grünwald-Giemsa-stained isolated cells at 10x magnification from a patient with colorectal cancer.

Assessment of direct cellular toxicity in the CT26 cell line.

CT26 murine colon carcinoma cells (ATCC) were diluted in complete culture medium (RPMI 1640 supplemented with 10% fetal calf serum and 2% glutamine/penicillin-streptomycin) and seeded at 500 cells per well into 384-well Corning plates (cat. no. 3764; Thermo Fisher Scientific, Inc.). Plates were incubated for 24 h at 37°C in a humidified atmosphere containing 5% CO₂. Mbz, cisplatin and gemcitabine were tested at the concentrations detailed above and were dispensed using an Echo 650 (Backman Coulter, Inc), followed by a 72 h incubation period in a 37°C humidified atmosphere containing 5% CO₂. After incubation, the plates were centrifuged (200 x g, 5 min, RT) and the supernatant was removed using an ELx405 plate washer. CellTiter-Glo[®] 2.0 reagent (25 µl/well; cat. no. G9243; Promega Corporation) was added using the Biomek 4000 liquid handling system. Plates were sealed, wrapped in foil, shaken (600 rpm for 2 min) and incubated in the dark for 10 min. Luminescence was then measured using a FLUOstar Omega microplate reader (BMG Labtech GmbH). The ATP-based viability method was chosen over the FMCA, as CT26 cells exhibit a pronounced fibroblast-like phenotype that may interfere with fluorescence-based viability measurements (36).

Drug interaction analysis ex vivo. The interaction between Mbz and cisplatin (0.37-30 µM), irinotecan (2.2-180 µM) or gemcitabine (1.1-90 µM) in solid tumor samples was assessed by comparing the SI for each drug separately and when combined with Mbz at 5 µM, a concentration that induced modest cytotoxicity alone. The drug concentration ranges used were previously shown to induce a suitable range of cytotoxic effects in solid tumor samples.

For the assessment of drug interaction for each drug and sample SI, area under the curve (AUC) was calculated. AUC_i was defined as the AUC_{Combo}/AUC_{Single} ratio, where AUC_{Combo} denotes the area under the concentration-SI curve for the drug combined with Mbz and AUC_{Single} denotes the AUC for the cytotoxic drug alone, as illustrated in Fig. 2. Thus, AUC_i ratios ≤ 1 indicate positive interactions (such as sub-additive or synergistic), whereas ratios > 1 indicate negative interactions (such as antagonistic). The results are illustrated by heatmaps plotted using the 'pheatmap' (version 1.0.12) package in R

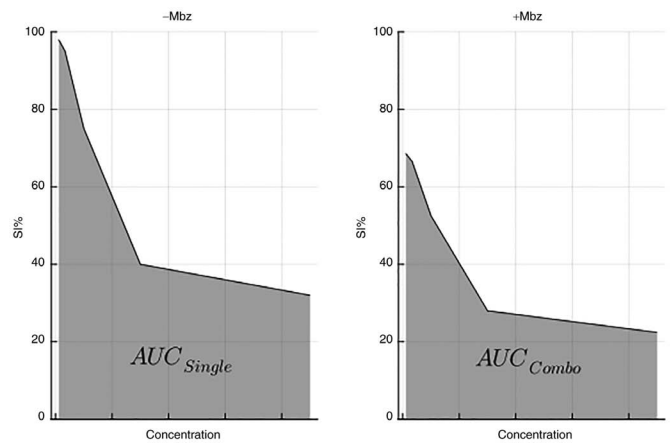


Figure 2. Schematic illustration of the *ex vivo* SI AUC for drugs alone and when combined with 5 µM Mbz. Calculation of the AUC ratios (AUC_{Combo}/AUC_{Single}) were used for the assessment of drug interactions *ex vivo*. SI, survival index; AUC, area under the curve; Mbz, mebendazole.

(<https://www.r-project.org>; version 4.1.2), with rows and columns ordered by hierarchical clustering (average linkage and Euclidean distance).

To further detail the interactions between Mbz and irinotecan or cisplatin, FMCA experiments were performed using 4 CRC samples and analyzed in SynergyFinder 3.0 (<https://synergyfinder.fimm.fi>), an online web-application that enables analysis and visualization of multi-drug combination screening data (37,38). The application offers interaction analysis with different models: Loewe additivity (39), Bliss excess (40), Zero Interaction Potency (ZIP) (41) and Highest Single Agent (HSA) (42). The interactions are visualized as two-dimensional heatmaps and then summarized over a dose-response matrix as an interaction score calculated for each interaction model. The synergy experiments were performed in triplicate.

Antitumor activity of Mbz and irinotecan in vivo. The animal care and *in vivo* experimental procedures were performed by Adlego Biomedical AB (Solna, Sweden) according to Good Laboratory Practice standards and per ethical approval by the regional animal ethics committee in Stockholm, Sweden (approval no. 12201-2019). The study started late 2021 and was finalized, including subsequent analyses in our laboratory, late 2022.

In total, 54 female BALB/c mice aged 6-7 weeks at arrival were obtained from Charles River Laboratories, Inc. The animals were kept 4-5 animals/cage in individually ventilated cages (type IVC 4). Bedding was provided by BeeKay Scanbur AB and all of the cages were enriched with happy homes, play tunnels, sizzle nest and soft paper wool (Scanbur AB). The mice were kept at 22±3°C with 50±20% humidity. Lighting was regulated to 12-h light and dark cycles and the animals had free access to food and water (RM 3; Special Diet Services). Animals weighed 17.0-18.4 g at arrival and 19.3-21.2 g on day 20 with no obvious differences between groups.

CT26, a murine colorectal carcinoma cell line derived from the BALB/c strain, was purchased from ATCC. Irinotecan was purchased from Fresenius Kabi AG and Mbz was purchased from Recipharm AB. On Day-11, animals were inoculated with

Table I. Treatment schedules for the experimental groups.

Compound	Administration route	Dose (mg/kg)	Schedule
Saline	i.v.	-	Twice weekly
LD Mbz	p.o.	20	Five times/week
HD Mbz	p.o.	50	Five times/week
Irinotecan	i.p.	15	Once weekly
Irinotecan + LD Mbz	i.p./p.o.	15+20	Once weekly + five times/week
Irinotecan + HD Mbz	i.p./p.o.	15+50	Once weekly + five times/week

i.v, intravenous; p.o., per-oral; i.p., intraperitoneal; HD, high dose; LD, low dose; Mbz, mebendazole.

3×10^5 CT26 cells (diluted in complete RPMI 1640 medium to a total volume of 100 μ l), subcutaneously in the right rear flank. Tumor volumes, body weights and the animal general health status were measured 3 times weekly by designated animal house technicians. In addition, the team conducting the experiments monitored the animals on each day of treatment and during the endpoint procedures. Tumor volumes (in mm^3) were measured using a caliper and calculated by the following formula: Length x width x width x0.44.

On Day-1, when the tumors had reached a mean volume of $46.5 \pm 1.97 \text{ mm}^3$, the animals were stratified into 6 experimental groups, with 9 animals per group. Treatment was then started at day 0, as detailed in Table I. The dosing schedule was aimed to be as clinically relevant as possible with Mbz considered to be a drug continuously administered orally and irinotecan intermittently intravenously, each at doses giving effects allowing for analysis of interactions (5,43). Treatment was to be continued for a maximum of 41 days after which the animals were euthanized by cervical dislocation. Animals with tumors $>2,000 \text{ mm}^3$ and/or tumor-related wounds, were to be euthanized pre-term in accordance with the ethical permit governing these experiments. For this reason, most animals were euthanized around day 20, thus tumor growth data are presented up until that day. Survival was defined as time from stratification to pre-term termination or day 41. Following euthanasia, tumors were extracted and placed in medium (CO_2 Independent Medium) with 5% heat-inactivated fetal calf serum (Sigma-Aldrich; Merck KGaA) and 1.1% glutamine/penicillin-streptomycin consisting of equal parts 200 mM L-glutamine (Sigma-Aldrich; Merck KGaA) and penicillin-streptomycin (10,000 U/ml penicillin and 10 mg/ml streptomycin in 0.9% NaCl; Sigma-Aldrich; Merck KGaA) and shipped directly to our laboratory for preparation of the cells for flow cytometric evaluation.

Flow cytometry. Immune cell infiltration in the mouse tumors was assessed by flow cytometry. Mouse tumor tissues were prepared by mechanical disintegration and collagenase digestion as aforementioned. Cells were then enriched for CD45⁺ expression using an AutoMACS Pro (Miltenyi Biotec GmbH).

Prior to flow cytometry analysis, the cells were washed and diluted with PBS (Thermo Fisher Scientific, Inc.) and human serum albumin (Sigma-Aldrich; Merck KGaA) (PBS-HSA) 0.1% for 5 min at 4°C. Gating antibodies were added to the cells according to the following: i) Macrophage panel: Lymphocyte

antigen 6 complex, locus G FITC (cat. no. 127605; Biolegend, Inc.), CD45 Pacific Orange (cat. no. MCD4530; Thermo Fisher Scientific, Inc.), CD163 PE (cat. no. 156704; Biolegend, Inc.), CD38 Pacific blue (cat. no. 102720; Biolegend, Inc.), F4/80 PE/Cy7 (cat. no. 123114; Biolegend, Inc.) and CD11b Violet 711 (cat. no. 101241; Biolegend, Inc.); and ii) T cell panel: CD8 FITC/CD4 PE/CD3 PC7 (cat. no. 558391; BD Biosciences) and CD45 Pacific Orange. All antibodies were diluted in PBS-HSA 0.1%. The cell and antibody mixture was incubated for 20 min in the dark, washed with cold 1% PBS-HSA and centrifuged at 400 x g for 5 min at 4°C. Finally, flow cytometry was performed using a Navios flow cytometer (Beckman Coulter, Inc.) and data were analyzed using Navios software v1.2 (Beckman Coulter, Inc.).

Statistical analysis. Statistical analysis was performed using GraphPad Prism™ 6 (Dotmatics). Between group differences were first analyzed by one-way ANOVA and if statistically significant, comparisons between groups were made using Dunnett's post hoc test. $P < 0.05$ was considered to indicate a statistically significant difference. The data are presented as mean \pm SD throughout.

Results

Mbz shows modest cytotoxicity in patient tumor cells ex vivo. In total, 222 patient samples fulfilled the FMCA quality criteria including AML (n=24) and ovarian (n=78), colorectal (n=71) and renal (n=49) cancer samples. The single-drug effect of Mbz was modest across all tumor types, with AML showing the highest sensitivity, followed by ovarian, colorectal and renal cancer (Fig. 3). Statistical analysis confirmed a significant difference between AML and CRC at the two highest concentrations ($P < 0.001$). Moreover, a significant difference was observed between AML and renal cell carcinoma at all tested concentrations except the lowest ($P < 0.001$ for the two highest concentrations and $P < 0.05$ for the remaining concentrations). Mbz had a modest effect at 5 μM (mean SI% 72, 76, 83 and 88 in AML, ovarian, colorectal and renal cancer, respectively) and this concentration was selected for the combination experiments.

Mbz enhances the effect of cytotoxic drugs in patient tumor cells. Drug interactions notably differed between samples and tumor types (Fig. 4). In all of the samples (n=82), regardless

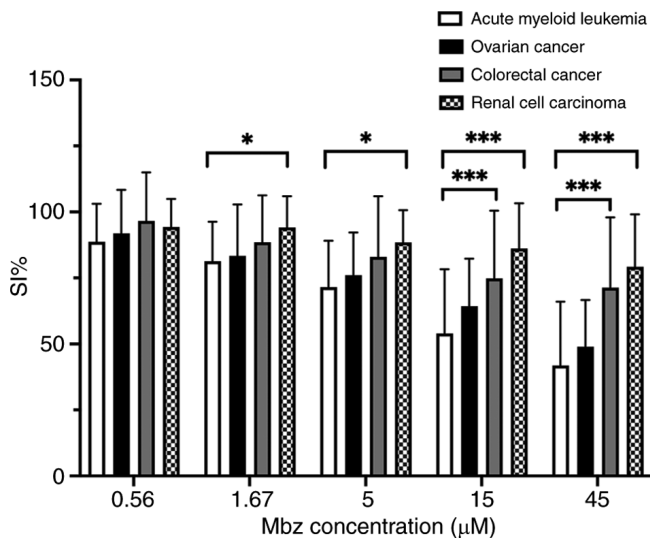


Figure 3. SI of *ex vivo* patient tumor cells exposed to the indicated Mzb concentrations for 72 h in (A) acute myeloid leukemia (n=24), (B) ovarian cancer (n=78), (C) colorectal cancer (n=71) and (D) renal cell cancer (n=49). Data are presented as mean \pm SD. *P<0.05, ***P<0.001 compared with acute myeloid leukemia. SI, survival index; Mzb, mebendazole.

of diagnosis, a positive interaction following the addition of Mzb was observed in 68% of the samples (50/74) for cisplatin, 77% (58/75) for gemcitabine and in 88% (72/82) for irinotecan. The corresponding numbers for renal cancer were 73% (14/19), 79% (15/19) and 85% (18/21), for ovarian cancer 64% (25/39), 68% (28/41) and 90% (38/42) and for CRC 84% (16/19), 69% (12/16) and 93% (14/15). Notably, some drug-sample combinations were not tested in all experiments (indicated in grey in Fig. 4), which explains why the sum of subgroup analyses does not equal the total number of samples.

To investigate the observed interactions between Mzb and irinotecan or cisplatin in more detail, a new set of FMCA experiments with 4 CRC samples were performed using the SynergyFinder application with four models for drug interactions. According to the application, interaction scores in the -10 to +10 range suggests additive interactions, >+10 synergistic and <-10 antagonistic interactions (36). The interaction scores for each patient and each interaction model are shown in Fig. 5. Overall, the interaction scores for the Mzb/irinotecan combination were higher across most interaction models compared with the Mzb/cisplatin combination, suggesting the Mzb/irinotecan combination to be the most favorable. Therefore, this combination was selected for the *in vivo* study. The majority of synergy scores for both combinations fell within the range of -10 to +10, indicating additive effects. However, the Mzb/irinotecan combinations occasionally exceeded +10 in certain models and samples, suggesting potential synergistic interactions.

Using Mann-Whitney test, a statistically significantly higher overall mean score was observed for the Mzb/irinotecan combination compared with the Mzb/cisplatin combination [mean synergy score for Mzb/irinotecan, 2.63 (Bliss excess, 2.11; HSA, 3.48; Loewe additivity, 2.63; ZIP, 2.32) vs. mean synergy score for Mzb/cisplatin, -2.69 (Bliss excess, -4.11; HSA, -1.16; Loewe additivity, -2.12; ZIP, -3.37); P<0.0001; Fig. 5].

The low synergy scores for the Mzb/cisplatin combination in sample 1 likely reflect the intrinsic drug sensitivity and resistance of that particular tumor sample. Individual tumor samples exhibit substantial heterogeneity in drug response, which underscores the value of using a patient-derived cell model to reflect drug activity in the clinic.

Cytotoxic effects in the CT26 murine colon cancer cell line in vitro. As a basis for the assessment of drug interactions *in vivo*, a corresponding set of experiments with *in vitro* CT26 cells were conducted using Mzb alone and in combination with cisplatin or irinotecan. Mzb alone showed a modest and an almost concentration independent activity (Fig. S1A), whereas both cisplatin and irinotecan induced a dose-dependent cytotoxicity (Fig. S1A and B). Furthermore, Mzb at 5 μ M enhanced the cytotoxic effect of cisplatin and irinotecan in an additive/sub-additive pattern without notable differences between these drugs (Fig. S1A-C).

Mzb inhibits tumor growth in the CT26 murine colon cancer model. Animal body weight and health status assessments showed that drug administration was not associated with a decrease in overall animal health status. Tumor growth was rapid and some animals (1-3 animals in each group) developed tumor-related wounds and were thus euthanized prior to the final study day. Tumor-related wound development was evenly distributed throughout groups and likely not correlated to drug administration. The maximum measured tumor diameter and volume were 17.6 mm and 2,877 mm³, respectively.

The mean tumor volumes for the control and experimental groups are shown in Fig. 6, divided into a and b for clarity. The values are presented up until day 13 for the control group as after this day most animals in this group had been euthanized pre-term, in accordance with the study protocol due to tumor growth, whereas most animals in the experimental groups were continued to day 20. At day 13, the control group had a mean tumor volume of 651 mm³ compared with 488 mm³ in the low dose Mzb group and 353 mm³ in the high dose Mzb group. The mean tumor volume at day 13 in animals treated with irinotecan was 523 mm³ and when irinotecan was combined with low or high dose Mzb, the volumes were 402 mm³ and 472 mm³, respectively. Differences between the groups were not statically significant. At day 20, the mean tumor volume in the irinotecan group was 1,533 mm³, the low dose Mzb group was 1,133 mm³ and the high dose Mzb group was 517 mm³. The tumor volume for irinotecan combined with low dose Mzb at day 20 was 737 mm³ and 699 mm³ for high dose Mzb. Compared with irinotecan alone, the differences were not statistically significant. At day 20, the difference between all groups was statistically significant according to one-way ANOVA (P=0.048), but only the difference between the mean tumor volumes in the irinotecan and high dose Mzb groups was statistically significant following post hoc test (P=0.04).

Kaplan Meier survival curves are presented in Fig. 7. Drug exposed animals showed a longer survival compared with the control animals. Control animals had a median survival time of 13 days, compared with 20-29 days for those drugs exposed. In agreement with the effect on tumor volumes, a dose-dependent effect of Mzb alone was indicated, with a median survival time of 20 days in animals treated with low

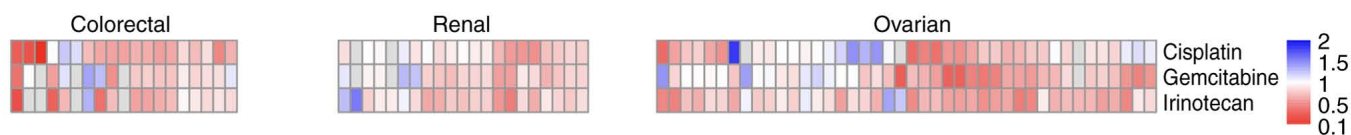


Figure 4. Heatmap of the *ex vivo* relative sensitivity of individual samples of patient tumor cells to 5 μM mebendazole in combination with cisplatin, gemcitabine or irinotecan, for each diagnosis indicated. Values <1 indicate subadditivity (synergy) and values >1 indicate antagonism.

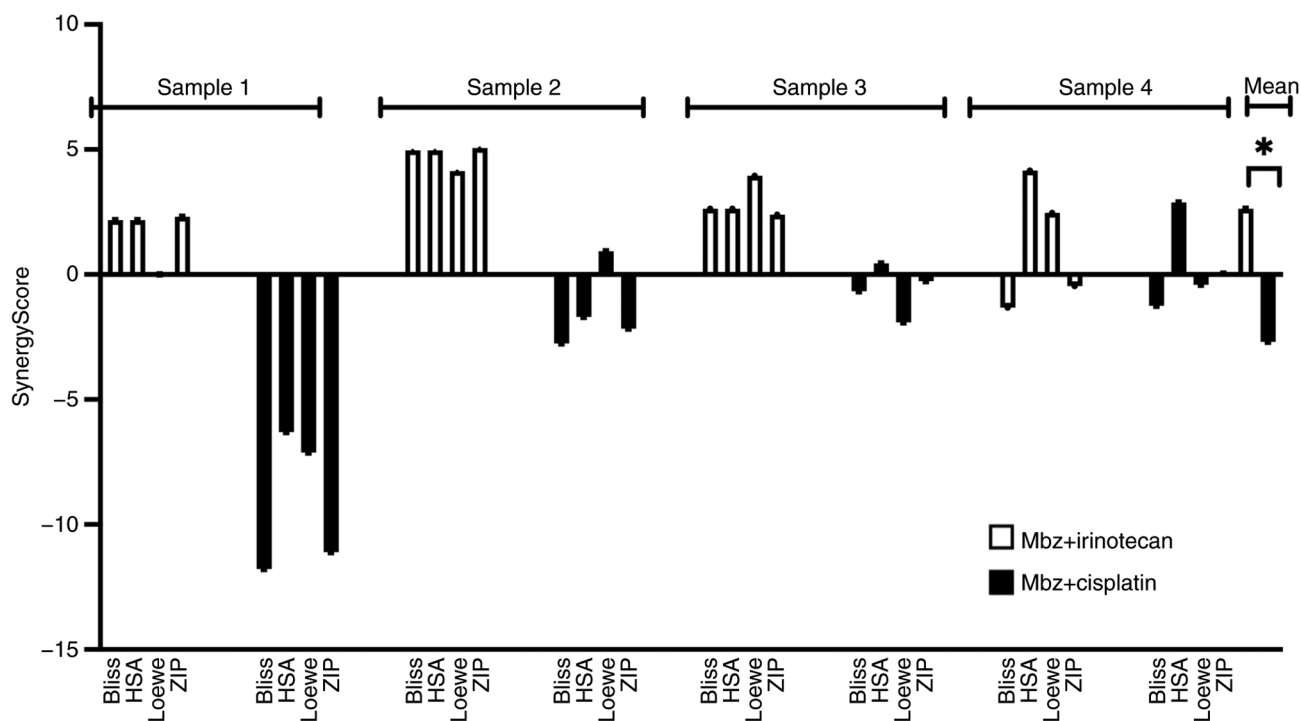


Figure 5. Distribution of the interaction scores calculated by SynergyFinder in 4 samples of colorectal cancer for Mbz combined with irinotecan or cisplatin, and for each of the four interaction models indicated. Scores in the -10 to +10 range suggest additive interaction, >10 synergistic and <-10 antagonistic interaction. *P<0.05. Mbz, mebendazole; Bliss, Bliss excess; HSA, Highest Single Agent; Loewe, Loewe additivity; ZIP, Zero Interaction Potency.

dose Mbz compared with 29 days for high dose Mbz. Animals treated with irinotecan combined with low or high dose Mbz had median survival times of 27 days.

Mbz modulates tumor immune cell infiltration in vivo. Based on our previous *ex vivo* findings of an immunomodulatory effect of Mbz switching macrophages from the M2 to M1 type (14,16), tumor tissue from the animals was retrieved and analyzed by flow cytometry to detect the presence of various subsets of immune cells. CD45⁺ cells were sorted for CD4⁺/CD8⁺ T cells, and macrophages were then classified further as type M1 (CD38⁺/CD80⁺) or type M2 (CD206⁺). Figs. S2-S7 illustrate the gating strategies used to identify macrophages and T cells, for each group separately.

Overall, Mbz slightly increased the infiltration of macrophages and CD4⁺ T cells (Fig. 8A and B). Mbz tended to dose-dependently increase the levels of M1 macrophages and decrease M2 macrophages (Fig. 8D-F). Thus, the mean M1/M2 ratio for low and high dose Mbz were 0.26 (range, 0.15-1.09) and 1.35 (range, 0.12-5.22), respectively, compared with 0.25 (range, 0.08-0.78) for the control group.

Mbz in combination with irinotecan increased the M1/M2 ratio, but not beyond the effect of Mbz alone. Irinotecan alone

seemingly increased the macrophage infiltration but otherwise did not notably alter the immune cell infiltration. The tumor immune cell data exhibited substantial variability and no statistically significant differences were observed between groups, except for CD8⁺ T cells. A significant increase in CD8⁺ T cells was observed in the high dose Mbz + irinotecan group compared with the control, low dose Mbz + irinotecan, low dose Mbz and irinotecan alone groups (P=0.01; Fig. 8C).

Discussion

Ex vivo drug sensitivity testing of primary cultures of tumor cells from patients using FMCA has previously shown a good correlation with clinical outcomes in several tumor types (44-47). Using this model in the present study, it was demonstrated that Mbz alone had a modest direct cytotoxic activity, in agreement with the general chemotherapeutic drug sensitivity known from our previous *ex vivo* characterization and from the clinic (2,3,48,49). This finding is in contrast to that observed in various cell line models, in which Mbz alone exhibits strong cytotoxic activity (2-7). However, cell lines have several limitations as tumor models and generally do not adequately reproduce drug sensitivity in the clinic

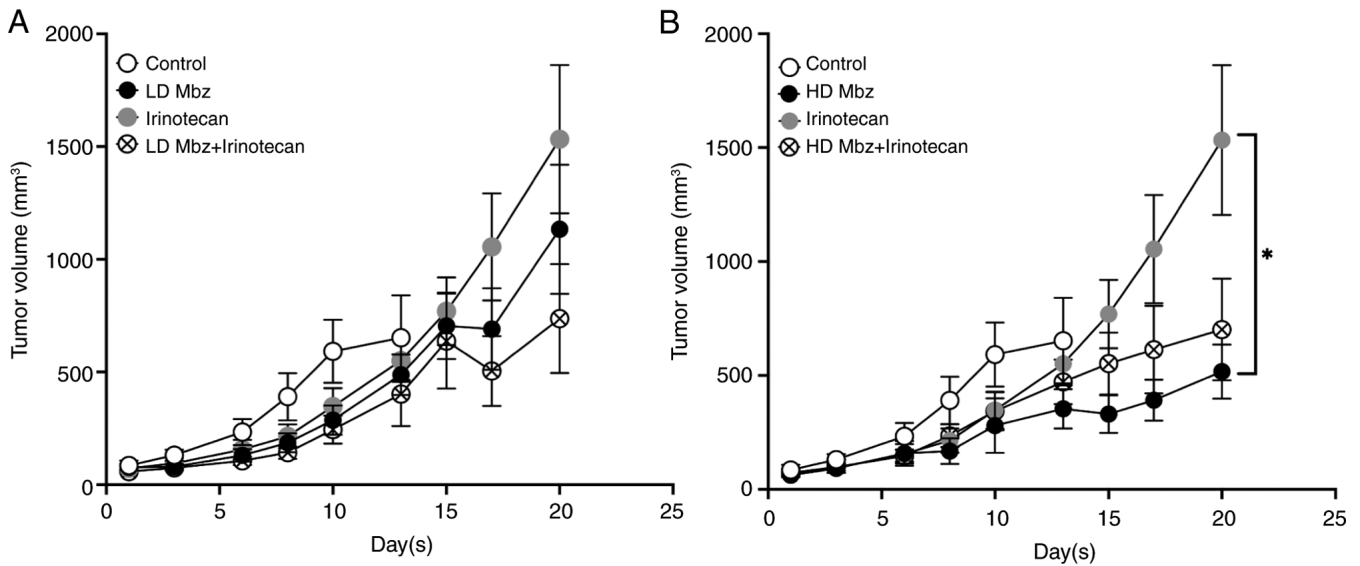


Figure 6. Tumor volumes over time in (A) mice exposed to LD Mbz or (B) HD Mbz and their combinations with irinotecan as well as effect of this drug alone. Treatment was started at day 0. The control group (saline) is only presented up to day 13 since most of the animals in this group had been euthanized beyond that day. Results are presented as mean \pm SD. * $P < 0.05$. LD, low dose; HD, high dose; Mbz, mebendazole.

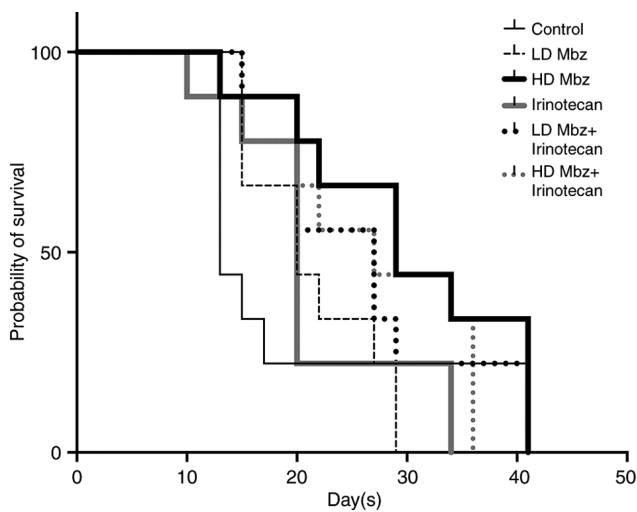


Figure 7. Kaplan-Meier survival curves for the control and experimental group mice. LD, low dose; HD, high dose; Mbz, mebendazole.

(50,51), in contrast to primary cultures of tumor cells from patients (50). Nevertheless, it should be acknowledged that single-cell culture models, including patient-derived cells, lack the complex interactions with immune cells and extracellular matrix components that are present in the *in vivo* tumor microenvironment.

Several mechanisms for a direct tumor cell Mbz cytotoxicity have been reported (52) such as tubulin polymerization inhibition (6), protein kinase inhibition (11), anti-angiogenesis (12) and inhibition of the Hedgehog pathway (13), and are considered notable for an anticancer drug. Together with the very advantageous safety profile of Mbz, these observations have fueled an interest in trying single drug Mbz for cancer treatment in patients. Mbz has been reported to induce tumor remission in case reports of patients with neuroendocrine

and colon cancer (9,10). Furthermore, in early clinical trials with patients with brain tumors, Mbz at higher dose (up to 200 mg/kg/day) seemingly stops tumor progression (28). Such observations are in line with the observed Mbz-induced tumor growth inhibition in different mouse models (2,5) and are corroborated by the dose-dependent inhibition of tumor growth observed in the *in vivo* CT26 colon cancer model in the present study.

However, the aforementioned findings contrast with our phase II clinical trial of last line, individualized, single drug Mbz in patients with advanced gastrointestinal cancer (26). In the trial, no objective tumor response to single-agent Mbz was observed, and a subset of patients showed unusually rapid disease progression, suggestive of hyperprogression, a phenomenon reported in patients treated with immune checkpoint inhibitors (53). Although it cannot be concluded that Mbz directly induced hyperprogression, one possible explanation is that Mbz modulates the immune system in a complex, context-dependent manner. While Mbz can promote pro-inflammatory responses in controlled *ex vivo* settings (16), the tumor microenvironment in patients, particularly in heavily pre-treated and immunosuppressed individuals, may respond differently.

The concept of combining several drugs remains a cornerstone of cancer therapy. This approach generally improves the benefit-risk balance compared with single drug treatment (17,18). Traditionally, anticancer drug combinations were established empirically, focusing on identifying regimens with non-overlapping toxicities. More recently, however, combination strategies are increasingly guided by mechanistic rationale based on tumor biology (19,20). Preclinical studies frequently report synergistic interactions when combining drugs whereas such interactions hardly apply in the clinic (21). Instead, additive or sub-additive interactions are more common and can still yield clinically meaningful benefits (22). Given the benefits of drug combinations and the negative results from

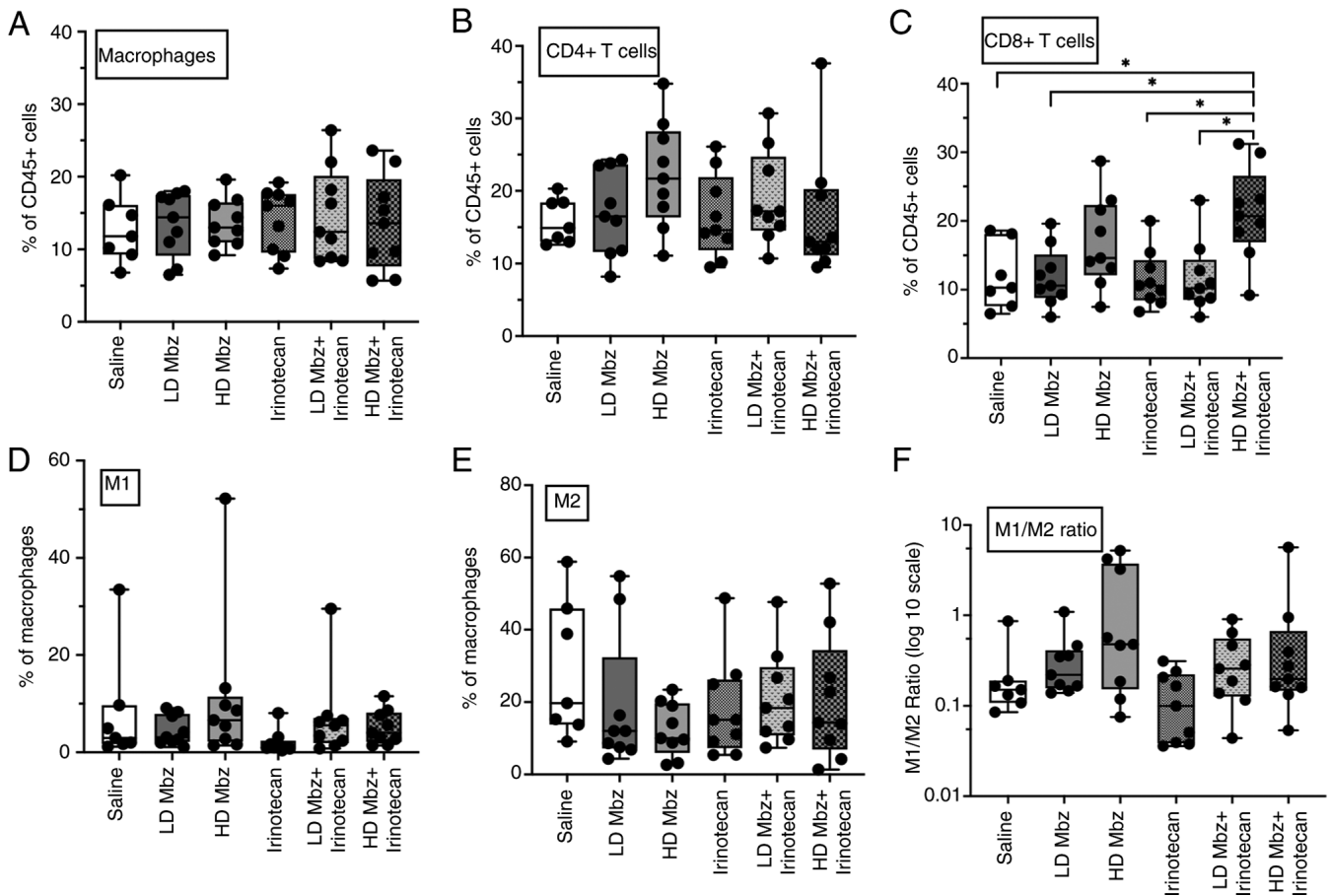


Figure 8. Box-and-whiskers plots presenting the immune cell populations in control and experimental group mice measured by flow cytometry. (A) Total macrophages, (B) CD4⁺ T cells, (C) CD8⁺ T cells, (D) M1 macrophages, (E) M2 macrophages and (F) M1/M2 ratio. Boxes encompass 50% of the observations, the horizontal line in box is the mean from 9 tumors analyzed and the whiskers indicate the observation ranges. The M1/M2 ratio data is presented by log₁₀ scale. *P<0.05. LD, low dose; HD, high dose; Mbz, mebendazole.

our aforementioned single-drug Mbz clinical trial, it is notable that a recent randomized study reported improved outcomes in advanced CRC when Mbz was combined with standard chemotherapy (FOLFOX) compared with chemotherapy alone (27). This finding prompted the investigation of the effect of Mbz combined with mechanistically different standard cytotoxic drugs in the present study. In patient tumor and CT26 cells, positive interactions in the sub-additive to additive range were observed, with the strongest effect noted for Mbz combined with irinotecan in patient cells. This finding suggests that the Mbz/irinotecan combination may be suitable for clinical testing, particularly in tumor types where irinotecan is part of the standard treatment, such as CRC.

In the present study, the observed positive interaction between Mbz and irinotecan was partly corroborated in the CT26 colon cancer mouse model. Low dose Mbz combined with irinotecan was more active than each drug individually, although this result was not statistically significant. By contrast, high dose Mbz combined with irinotecan tended to be less active than Mbz alone. The reason for this seemingly dose-dependent interaction difference is unclear. However, it could be speculated that the stronger tumor growth inhibition from high dose Mbz compared with low dose Mbz was reduced by irinotecan-induced counteracting changes in the tumor macrophage infiltration.

From a clinical point of view, the observations of the present study make the selection of candidate Mbz combinations for clinical testing complicated. If the anticancer effect of Mbz *in vivo* is mainly due to changes in tumor immune cell infiltration, screening of drugs suitable for combination with Mbz using cell lines or patient-derived primary culture models will not produce data applicable *in vivo*. Other models that also reflect drug effects on immune cells would be necessary to select drugs appropriate for combination with Mbz. Notably, Mbz has been successfully combined with FOLFOX in treating CRC (27), but has also been combined with bevacizumab, irinotecan, temozolomide or lomustine in early clinical trials of patients with brain tumors (28-30). The antitumor activity in these trials was seemingly very modest and the trial design did not allow for any conclusions on whether these combinations were justified from a mechanistic point of view. In this context, combination of Mbz with other immunomodulatory drugs is conceptually interesting. Indeed, preliminary results in our laboratory from *in vivo* experiments of the CT26 model treated with an immune checkpoint inhibiting antibody indicate a positive interaction with Mbz. Another important avenue in repurposing Mbz for use in cancer therapy is the development of drug carriers or prodrugs to overcome the pharmacokinetic issues associated with Mbz (54).

One strength of the present study is the use of primary cultures of patient tumor cells, a model known to better reflect clinical outcomes than tumor cell lines (55). While the findings of the present study provide valuable insights into the anti-cancer properties of Mbz, the limitations of the study should be acknowledged. The *ex vivo*, *in vivo* and *in vitro* models utilized do not recapitulate the complexity of cancer, necessitating further validation in preclinical and clinical models.

In conclusion, the present study highlights the multifaceted anticancer properties of Mbz. Thus, findings from this and other published studies suggest that a key mechanism of the anticancer effect of Mbz may be immune modulation in addition to direct cytotoxicity. It would be of interest to explore whether pharmacological agents known to promote M1 to M2 macrophage polarization might antagonize the effects of Mbz. Such studies could provide valuable insights into the immunomodulatory role of Mbz and inform on combination strategies. However, selection of the best drugs to combine with Mbz for efficacy optimization requires careful consideration based on further research.

Acknowledgements

Not applicable.

Funding

This study was supported by grants from The Swedish Cancer Society (grant nos. 14 445, 17 0661 and 20 844) and The Cancer Research Fund at the Uppsala University hospital (grant no. 2022-PN).

Availability of data and materials

The data generated in the present study may be requested from the corresponding author.

Authors' contributions

The study was designed and performed with significant contributions from all authors. SM, CA, PN, MF and RL conceptualized and designed the study. SM and KB performed the experiments and collected the data. SM, KB, CA and PN analyzed the data. SM and PN wrote the manuscript. KB, CA, MF and RL revised the manuscript. SM and PN confirm the authenticity of all the raw data. All authors read and approved the final version of the manuscript.

Ethics approval and consent to participate

The collection of patient tumor samples was approved from the Swedish Ethics Review Board (approval no. 2007/237). Written informed consent for sample collection and further analysis was provided by all patients before sample collection. The *in vivo* experiments were approved by the regional animal ethics committee in Stockholm (approval no. 12201-2019).

Patient consent for publication

Written patient consent for tumor sampling also included the publication of results.

Competing interests

RL, PN and MF are co-founders and shareholders of Repos Pharma AB, a Swedish research and development company dedicated to investigations of drug repositioning. Repos Pharma AB was not involved in the study design, execution, data analysis or writing of the manuscript. The remaining authors declare that they have no competing interests.

References

- Pantziarka P, Bouche G, Meheus L, Sukhatme V and Sukhatme VP: Repurposing drugs in oncology (ReDO)-mebendazole as an anti-cancer agent. *Ecancermedicallscience* 8: 443, 2014.
- Mukhopadhyay T, Sasaki J, Ramesh R and Roth JA: Mebendazole elicits a potent antitumor effect on human cancer cell lines both *in vitro* and *in vivo*. *Clin Cancer Res* 8: 2963-2969, 2002.
- Martarelli D, Pompei P, Baldi C and Mazzoni G: Mebendazole inhibits growth of human adrenocortical carcinoma cell lines implanted in nude mice. *Cancer Chemother Pharmacol* 61: 809-817, 2008.
- Doudican NA, Byron SA, Pollock PM and Orlow SJ: XIAP downregulation accompanies mebendazole growth inhibition in melanoma xenografts. *Anticancer Drugs* 24: 181-188, 2013.
- Bai RY, Staedtke V, Aprhys CM, Gallia GL and Riggins GJ: Antiparasitic mebendazole shows survival benefit in 2 preclinical models of glioblastoma multiforme. *Neuro Oncol* 13: 974-982, 2011.
- Sasaki J, Ramesh R, Chada S, Gomyo Y, Roth JA and Mukhopadhyay T: The anthelmintic drug mebendazole induces mitotic arrest and apoptosis by depolymerizing tubulin in non-small cell lung cancer cells. *Mol Cancer Ther* 1: 1201-1209, 2002.
- Pourgholami MH, Cai ZY, Chu SW, Galettis P and Morris DL: The influence of ovarian cancer induced peritoneal carcinomatosis on the pharmacokinetics of albendazole in nude mice. *Anticancer Res* 30: 423-428, 2010.
- Aliabadi A, Haghshenas MR, Kiani R, Koochi-Hosseiniabadi O, Purkhosrow A, Pirsalami F, Panjehshahin MR and Erfani N: *In vitro* and *in vivo* anticancer activity of mebendazole in colon cancer: A promising drug repositioning. *Naunyn Schmiedeberg Arch Pharmacol* 397: 2379-2388, 2023.
- Nygren P and Larsson R: Drug repositioning from bench to bedside: Tumour remission by the anthelmintic drug mebendazole in refractory metastatic colon cancer. *Acta Oncol* 53: 427-428, 2014.
- Dobrosotskaya IY, Hammer GD, Scheingart DE, Maturen KE and Worden FP: Mebendazole monotherapy and long-term disease control in metastatic adrenocortical carcinoma. *Endocr Pract* 17: e59-e62, 2011.
- Nygren P, Fryknäs M, Agerup B and Larsson R: Repositioning of the anthelmintic drug mebendazole for the treatment of colon cancer. *J Cancer Res Clin Oncol* 139: 2133-2140, 2013.
- Bai RY, Staedtke V, Rudin CM, Bunz F and Riggins GJ: Effective treatment of diverse medulloblastoma models with mebendazole and its impact on tumor angiogenesis. *Neuro Oncol* 17: 545-554, 2015.
- Larsen AR, Bai RY, Chung JH, Borodovsky A, Rudin CM, Riggins GJ and Bunz F: Repurposing the anthelmintic mebendazole as a hedgehog inhibitor. *Mol Cancer Ther* 14: 3-13, 2015.
- Blom K, Rubin J, Berglund M, Jarvius M, Lenhammar L, Parrow V, Andersson C, Loskog A, Fryknäs M, Nygren P and Larsson R: Mebendazole-induced M1 polarisation of THP-1 macrophages may involve DYRK1B inhibition. *BMC Res Notes* 12: 234, 2019.
- Blom K, Senkowski W, Jarvius M, Berglund M, Rubin J, Lenhammar L, Parrow V, Andersson C, Loskog A, Fryknäs M, *et al*: The anticancer effect of mebendazole may be due to M1 monocyte/macrophage activation via ERK1/2 and TLR8-dependent inflammasome activation. *Immunopharmacol Immunotoxicol* 39: 199-210, 2017.
- Rubin J, Mansoori S, Blom K, Berglund M, Lenhammar L, Andersson C, Loskog A, Fryknäs M, Nygren P and Larsson R: Mebendazole stimulates CD14+ myeloid cells to enhance T-cell activation and tumour cell killing. *Oncotarget* 9: 30805-30813, 2018.

17. Bayat Mokhtari R, Homayouni TS, Baluch N, Morgatskaya E, Kumar S, Das B and Yeger H: Combination therapy in combating cancer. *Oncotarget* 8: 38022-38043, 2017.
18. Law MR, Wald NJ, Morris JK and Jordan RE: Value of low dose combination treatment with blood pressure lowering drugs: Analysis of 354 randomised trials. *BMJ* 326: 1427, 2003.
19. Foucquier J and Guedj M: Analysis of drug combinations: Current methodological landscape. *Pharmacol Res Perspect* 3: e00149, 2015.
20. Boshuizen J and Peeper DS: Rational cancer treatment combinations: An urgent clinical need. *Mol Cell* 78: 1002-1018, 2020.
21. Ocana A, Amir E, Yeung C, Seruga B and Tannock IF: How valid are claims for synergy in published clinical studies? *Ann Oncol* 23: 2161-2166, 2012.
22. Hwangbo H, Patterson SC, Dai A, Plana D and Palmer AC: Additivity predicts the efficacy of most approved combination therapies for advanced cancer. *Nat Cancer* 4: 1693-1704, 2023.
23. Simbulan-Rosenthal CM, Dakshanamurthy S, Gaur A, Chen YS, Fang HB, Abdussamad M, Zhou H, Zapas J, Calvert V, Petricoin EF, *et al*: The repurposed anthelmintic mebendazole in combination with trametinib suppresses refractory NRASQ61K melanoma. *Oncotarget* 8: 12576-12595, 2017.
24. Kipper FC, Silva AO, Marc AL, Confortin G, Junqueira AV, Neto EP and Lenz G: Vinblastine and anthelmintic mebendazole potentiate temozolomide in resistant gliomas. *Invest New Drugs* 36: 323-331, 2018.
25. Coyne CP, Jones T and Bear R: Gemcitabine-(C₄-amide)-[anti-HER2/neu] Anti-neoplastic cytotoxicity in dual combination with mebendazole against chemotherapeutic-resistant mammary adenocarcinoma. *J Clin Exp Oncol* 2: 1000109, 2013.
26. Mansoori S, Fryknäs M, Alvfors C, Loskog A, Larsson R and Nygren P: A phase 2a clinical study on the safety and efficacy of individualized dosed mebendazole in patients with advanced gastrointestinal cancer. *Sci Rep* 11: 8981, 2021.
27. Hegazy SK, El-Azab GA, Zakaria F, Mostafa MF and El-Ghoneimy RA: Mebendazole; from an anti-parasitic drug to a promising candidate for drug repurposing in colorectal cancer. *Life Sci* 299: 120536, 2022.
28. Gallia GL, Holdhoff M, Brem H, Joshi AD, Hann CL, Bai RY, Staedtke V, Blakeley JO, Sengupta S, Jarrell TC, *et al*: Mebendazole and temozolomide in patients with newly diagnosed high-grade gliomas: Results of a phase I clinical trial. *Neurooncol Adv* 3: vdaa154, 2020.
29. Krystal J, Hanson D, Donnelly D and Atlas M: A phase I study of mebendazole with bevacizumab and irinotecan in high-grade gliomas. *Pediatr Blood Cancer* 71: e30874, 2024.
30. Patil VM, Menon N, Chatterjee A, Tonse R, Choudhari A, Mahajan A, Puranik AD, Epari S, Jadhav M, Pathak S, *et al*: Mebendazole plus lomustine or temozolomide in patients with recurrent glioblastoma: A randomised open-label phase II trial. *EClinicalMedicine* 49: 101449, 2022.
31. Anand U, Dey A, Chandel AKS, Sanyal R, Mishra A, Pandey DK, Falco VD, Upadhyay A, Kandimalla R, Chaudhary A, *et al*: Cancer chemotherapy and beyond: Current status, drug candidate, associated risks and progress in targeted therapeutics. *Genes Disease* 10: 136-1401, 2022.
32. Blom K, Nygren P, Alvarsson J, Larsson R and Andersson CR: Ex vivo assessment of drug activity in patient tumor cells as a basis for tailored cancer therapy. *J Lab Autom* 21: 178-187, 2016.
33. Larsson R and Nygren P: Laboratory prediction of clinical chemotherapeutic drug resistance: A working model exemplified by acute leukaemia. *Eur J Cancer* 29A: 1208-1212, 1993.
34. Lindhagen E, Nygren P and Larsson R: The fluorometric microculture cytotoxicity assay. *Nat Protoc* 3: 1364-1369, 2008.
35. Karlsson H, Fryknäs M, Senkowski W, Larsson R and Nygren P: Selective radiosensitization by nitazoxanice of quiescent clonogenic colon cancer tumour cells. *Oncol Lett* 23: 123, 2022.
36. Miles FL, Lynch JE and Sikes RA: Cell-based assays using calcein acetoxymethyl ester show variation in fluorescence with treatment conditions. *J Biol Method* 2: e29, 2015.
37. Ianevski A, Giri AK and Aittokallio T: SynergyFinder 2.0: Visual analytics of Multi-drug combination synergies. *Nucleic Acids Res* 48: W488-W493, 2020.
38. Ianevski A, Giri AK and Aittokallio T: SynergyFinder 3.0: An interactive analysis and consensus interpretation of multi-drug synergies across multiple samples. *Nucleic Acids Res* 50: W739-W743, 2022.
39. Loewe S: The problem of synergism and antagonism of combined drugs. *Arzneimittelforschung* 3: 285-290, 1953.
40. Bliss CI: The toxicity of poisons applied jointly. *Ann Appl Biol* 26: 585-615, 1939.
41. Yadav B, Wennerberg K, Aittokallio T and Tang J: Searching for drug synergy in complex dose-Response landscapes using an interaction potency model. *Comput Struct Biotechnol J* 13: 504-513, 2015.
42. Berenbaum MC: What is synergy? *Pharmacol Rev* 41: 93-141, 1989.
43. Moon CH, Lee SJ, Lee HY, Lee JC, Cha H, Cho WJ, Park JW, Park HJ, Seo J, Lee YH, *et al*: KML001 displays vascular disrupting properties and irinotecan combined antitumor activities in a murine tumor model. *PLoS One* 8: e53900, 2013.
44. Csóka K, Tholander B, Gerdin E, de la Torre M, Larsson R and Nygren P: In vitro determination of cytotoxic drug response in ovarian carcinoma using the fluorometric microculture cytotoxicity assay (FMCA). *Int J Cancer* 72: 1008-1012, 1997.
45. von Heideman A, Tholander B, Grundmark B, Cajander S, Gerdin E, Holm L, Axelsson A, Rosenberg P, Mahteme H, Daniel E, *et al*: Chemotherapeutic drug sensitivity of primary cultures of epithelial ovarian cancer cells from patients in relation to tumour characteristics and therapeutic outcome. *Acta Oncol* 53: 242-250, 2014.
46. Cashin PH, Söderström M, Blom K, Artursson S, Andersson C, Larsson R and Nygren P: Ex vivo assessment of chemotherapy sensitivity of colorectal cancer peritoneal metastases. *Br J Surg* 110: 1080-1083, 2023.
47. Bjersand K, Blom K, Poromaa IS, Stålberg K, Lejon AM, Bäckman F, Nyberg Å, Andersson C, Larsson R and Nygren P: Ex vivo assessment of cancer drug sensitivity in epithelial ovarian cancer and its association with histopathological type, treatment history and clinical outcome. *Int J Oncol* 61: 128, 2022.
48. Zhang X, Zhao J, Gao X, Pei D and Gao C: Anthelmintic drug albendazole arrests human gastric cancer cells at the mitotic phase and induces apoptosis. *Exp Ther Med* 13: 595-603, 2017.
49. Huang L, Zhao L, Zhang J, He F, Wang H, Liu Q, Shi D, Ni N, Wagstaff W, Chen C, *et al*: Antiparasitic mebendazole (MBZ) effectively overcomes cisplatin resistance in human ovarian cancer cells by inhibiting multiple cancer-associated signaling pathways. *Aging (Albany NY)* 13: 17407-17427, 2021.
50. Salvadores M, Fuster-Tormo F and Supek F: Matching cell lines with cancer type and subtype of origin via mutational, epigenomic, and transcriptomic patterns. *Sci Adv* 6: eaba1862, 2020.
51. Mirabelli P, Coppola L and Salvatore M: Cancer cell lines are useful model systems for medical research. *Cancers (Basel)* 11: 1098, 2019.
52. Guerini AE, Triggiani L, Maddalo M, Bonù ML, Frassinetti F, Baiguini A, Alghisi A, Tomasini D, Borghetti P, Pasinetti N, *et al*: Mebendazole as a candidate for drug repurposing in oncology: An extensive review of current literature. *Cancers (Basel)* 11: 1284, 2019.
53. Champiat S, Ferrara R, Massard C, Besse B, Marabelle A, Soria JC and Ferte C: Hyperprogressive disease: Recognizing a novel pattern to improve patient management. *Nat Rev Clin Oncol* 15: 748-762, 2018.
54. Abu-Hdaib B, Nsairat H, El-Tanani M, Al-Deeb I and Hasasna N: In vivo evaluation of mebendazole and Ran GTPase inhibition in breast cancer model system. *Nanomedicine (Lond)* 19: 1087-1101, 2024.
55. Idrisova K, Simon H and Gomzikova M: Role of patient-derived models of cancer in translational oncology. *Cancers* 15: 139, 2022.

